

| | | | | |
|---|--|---------|----------|--|
|  EPIDOT 125 Jahre Mineralfundstelle KNAPPENWAND NEUKIRCHEN AM GROSSVENEDIGER | 125 Jahre Knappenwand – 125 years Knappenwand Proceedings of a Symposium held in Neukirchen am Großvenediger (Salzburg/Austria) September 1990 | | | Editors: Volker Höck Friedrich Koller |
| Abh. Geol. B.-A. | ISSN 0378-0864 ISBN 3-900312-85-0 | Band 49 | S. 43–48 | Wien, Juni 1993 |

**Epidote and Associated Fissure Minerals
from Pfarrerb near Sobotín (Northern Moravia, Czech Republic):
A Manifestation of a Retrograde Phase
of the Variscan Regional Metamorphism**

By MILAN NOVÁK, VLADIMÍR ŠREIN & ANNA LANGROVÁ*)

With 3 Figures and 3 Tables

*Czech Republic
Sobotín (Zöptau)
Epidote
Mineralogy
Paragenesis
Variscan Metamorphism*

Contents

| | |
|---|----|
| Zusammenfassung | 43 |
| Abstract | 44 |
| 1. Introduction | 44 |
| 2. Occurrence and Mineral Parageneses | 44 |
| 3. Chemical Composition | 45 |
| 4. Discussion | 47 |
| Acknowledgement | 48 |
| References | 48 |

**Epidot und begleitende Kluftminerale
von Pfarrerb nahe Sobotín (Zöptau; Nordmähren, Tschechische Republik):
Ein Nachweis einer retrograden Phase
der variszischen Regionalmetamorphose**

Zusammenfassung

Epidot und begleitende Kluftminerale von Pfarrerb nahe Sobotín (Zöptau), Nordmähren, wurden untersucht. Sie treten in Metabasiten (wechselseitig ausgetauschten Amphibol-Albit-, Amphibol-Epidot- und Aktinolith-Epidot-Schiefern) des Sobotín-Massivs auf. Zwei unterschiedliche paragenetische Gruppen wurden festgestellt: Der Typ A entspricht der Mineralvergesellschaftung Diopsid – Aktinolith – Epidot – Albit – Laumontit – Desmin – Hornblende – Asbest sowie untergeordnet Kalifeldspat, Quarz, Titanit, Apatit und Prehnit. Der Typ P beinhaltet Diopsid – Apatit – Epidot I – Prehnit – Epidot II – Kalifeldspat sowie selten Titanit.

Sowohl die Zusammensetzung als auch der Zonarbau der Epidote aus beiden paragenetischen Gruppen sind unterschiedlich. Typ A Epidote besitzen ein X_{Fe} von 0.18–0.28 und eine geringfügige oder fehlende Zonierung mit Al- und Fe-reichen Rändern. Die Typ P Epidote zeigen einen intensiven Zonarbau und variieren von X_{Fe} 0.13–0.31. Die Diopside haben ein Mg/Mg+Fe-Verhältnis zwischen 0.76–0.82 bei einem Al_2O_3 -Gehalt von 0.70–1.50 Gew.-%. Aktinolith hat ein Mg/Mg+Fe von 0.68–0.75 mit 1.58–3.11 Gew.-% Al_2O_3 . Prehnit ist mit X_{Fe} Werten von 0.12–0.15 sehr einheitlich zusammengesetzt. Sowohl Albit als auch Kalifeldspat sind fast reine Endglieder der Mischungsreihen.

Die obere Temperatur-Stabilitätsgrenze für die Kluftmineralbildung liegt unter 350 bis 400°C bei einem Druck von P_{fluid} = 2–3 kbar. Das untere Temperaturlimit entspricht <150°C bei 1 kbar P_{fluid} . Die Unterschiede in Paragenese und Zonarbau in den Typen A und P werden durch unterschiedliche Fluids, die aus den angrenzenden Gesteinen stammen, verursacht. Der Typ P kann mit dem Zonarbau und der variablen Zusammensetzung der Epidote charakterisiert werden. Dies wird auf ein höheres fO_2 , zeitweise Änderungen in Temperatur, fO_2 und/oder pH zurückgeführt. In beiden Paragenesen waren die Fluids H_2O -reich und arm an CO_2 .

Die untersuchte Mineralisation wurde vermutlich während der retrograden variszischen Regionalmetamorphose gebildet. Zusammensetzung, Phasenbeziehung und Paragenese entsprechen weitgehend jener aus Metabasiten in Grünschiefer-Zeolith-Fazies mit einigen Ähnlichkeiten in den Epidot-führenden Klüften des aktiven Geothermalsystems von Salton Sea (Kalifornien).

*) Authors' addresses: MILAN NOVÁK, Department of Mineralogy and Petrography, Moravian Museum, Zelný trh 6, 659 37 Brno, Czech Republic; VLADIMÍR ŠREIN, ANNA LANGROVÁ, Geological Institution, Czech Academy of Sciences, Rozvojová 165, 165 00 Praha 6, Czech Republic.

Abstract

Epidote and associated fissure minerals from Pfarrerb near Sobotín, northern Moravia, were studied; they occur in metabasites (interbedded amphibole-albite, amphibole-epidote and actinolite-epidote schists and massive amphibolites) of the Sobotín massif. Two paragenetic types were recognized: the type A characterized by the sequence diopside-actinolite-epidote-albite-laumontite-stilbite-asbestos including rare K-feldspar, quartz, sphene, apatite and prehnite and the type P exhibited the sequence diopside – apatite – epidote I – prehnite – epidote II – K-feldspar including rare sphene. Composition and zoning pattern of epidote crystals from both paragenetic types are different. Type A epidote crystals vary composition from 0.18 to 0.28 X_{Fe} and show a weak to negligible zoning with Al-rich core and Fe-rich rim. Type P epidotes display wider composition range from 0.13 to 0.31 X_{Fe} and pronounced zoning of the same zonal trend. Diopside ranges from Mg/Mg+Fe ratio from 0.76 to 0.82 and Al_2O_3 content from 0.70 to 1.50 wt%; actinolite and Mg/Mg+Fe ratio from 0.68 to 0.75 and Al_2O_3 content from 1.58 to 3.11 wt%. Prehnite is chemically more uniform, the X_{Fe} value varies from 0.12 to 0.15 with Al-rich core. Both albite, K-feldspar are very close to their end-member compositions.

The upper temperature limit for fissure formation occurs below 350 to 400°C at $P_{fluid} = 2$ to 3 kbar; the lower limit may correspond to temperatures and pressures below 150°C and $P_{fluid} = 1$ kbar. Apparent differences in mineral parageneses and zoning pattern of epidote crystals between type A and type P reflect difference in composition and the fluids derived from closely adjacent rocks. High Na activity and lower fO_2 were associated with type A parageneses. The type P is characterized by wider compositional range and pronounced zoning of epidote; this may result from higher fO_2 and significant change in temperature, fO_2 and/or pH. In both paragenetic types fluids were enriched in H_2O with very low CO_2 activity.

The studied mineralization fissures most likely originated during a retrograde phase of the Variscan regional metamorphism. The observed mineral assemblage, paragenetic relations and compositional variations of minerals are very similar to those from metabasites of the greenschist to zeolite facies, and to a certain extent to epidote-bearing veins in active geothermal system within the Salton Sea, California.

1. Introduction

The most famous Moravian occurrence of fissure minerals at Pfarrerb nearby Sobotín (formerly named Zöptau) is situated in the southern part of the Hrubý Jeseník Mts. and in a region of the Sobotín metabasite massif. Previous mineralogical studies concerning mineral morphologies, parageneses and composition of epidote have been published in the second half of the last century (e.g. ZEPHAROVICH, 1865; von RATH, 1881; KRETSCHMER, 1895, 1911; NEUWIRTH, 1904). A brief contribution to chemistry of minerals and to mineral assemblages was recently given by NOVÁK (1990). In this paper, results of detailed study of parageneses and compositions of minerals especially epidote are discussed in order to elucidate P-T-X conditions for formation of the mineralized fissures.

2. Occurrence and Mineral Parageneses

The mineralized fissures occur in a metabasic complex in the centre of the Sobotín massif. The Devonian layered metabasites consist of interbedded amphibole-albite, amphibole-epidote and actinolite-epidote schists and massive amphibolites; they were metamorphosed during the Variscan regional metamorphism. This event is characterized by temperatures from 350 to 425°C (FIALA et al. 1980). However, RENÉ (1983) described some Variscan metapelites of the Desná Dome along the close north-western border of the Sobotín massif at significantly higher P-T conditions at P_{tot} of 5 to 7 kbar and temperature of 540 to 650°C.

The main fissure up to 30 cm thick and several meters long strike north to northwest; however, the strike and especially the dip of a single fissure may vary significantly (KRETSCHMER, 1895). At the contact between fissures and surrounding rocks occur strongly heterogeneous zone from several mm to about 10 cm thick consisting of coarse-grained actinolite, diopside and/or epidote. It is often broken by tectonic movements

and strongly weathered. Fissure minerals such as diopside, epidote or prehnite have been only very rarely found to be grown at this rock. Numerous small veinlets characterized by prevailing albite accompany the main fissures.

KRETSCHMER (1895) described six main mineralized fissures with contrasting mineral parageneses irregularly distributed within a small area; outcrops several meters distant from each other. The first paragenetic type A is characterized by common association of albite and epidote. In order of decreasing abundance, other minerals identified in this type are diopside, actinolite, actinolite-asbestos, K-feldspar, quartz, laumontite, stilbite, sphene, apatite and prehnite. The paragenetic type P is characterized by abundant prehnite and epidote with less amounts of diopside, apatite, K-feldspar actinolite-asbestos and sphene.

Paragenetic diagram of selected fissure minerals based on binocular and petrographic microscope studies is shown in Fig. 1. The earliest mineral diopside is often strongly corroded perhaps before the epidote formation in both paragenetic types. Actinolite was found in the type A and is rarely associated with epidote; it seems to have formed earlier. The sequence of formation of accessory phases such as sphene, quartz and K-feldspar in the type A is not clear. They appear younger than epidote, but perhaps older than albite; however, their relations are problematic. In both paragenetic types with a pale gray fine-fibrous actinolite-asbestos occur. Textural relations indicate that they formed later than epidote and actinolite; however, they might have formed during very broad temperature range even after the stilbite formation. Within the type P exceptionally rare second generations of fine-grained epidote II has been observed to be younger than prehnite. Calcite and chlorite, the typical fissure minerals occurring in similar localities as Knappenwand, Unter-

| Type A | Type P |
|---------------------|--------|
| DIOPSIDE | — |
| ACTINOLITE | — |
| EPIDOTE | — |
| ALBITE | — |
| LAUMONTITE | — |
| STILBITE | — |
| ACTINOLITE ASBESTOS | — — — |
| DIOPSIDE | — |
| APATITE | — |
| EPIDOTE I | — |
| PREHNITE | — |
| EPIDOTE II | — |
| K-FELDSPAR | — |
| ACTINOLITE ASBESTOS | — — — |

Fig. 1.
Paragenetic diagram of selected fissure minerals.

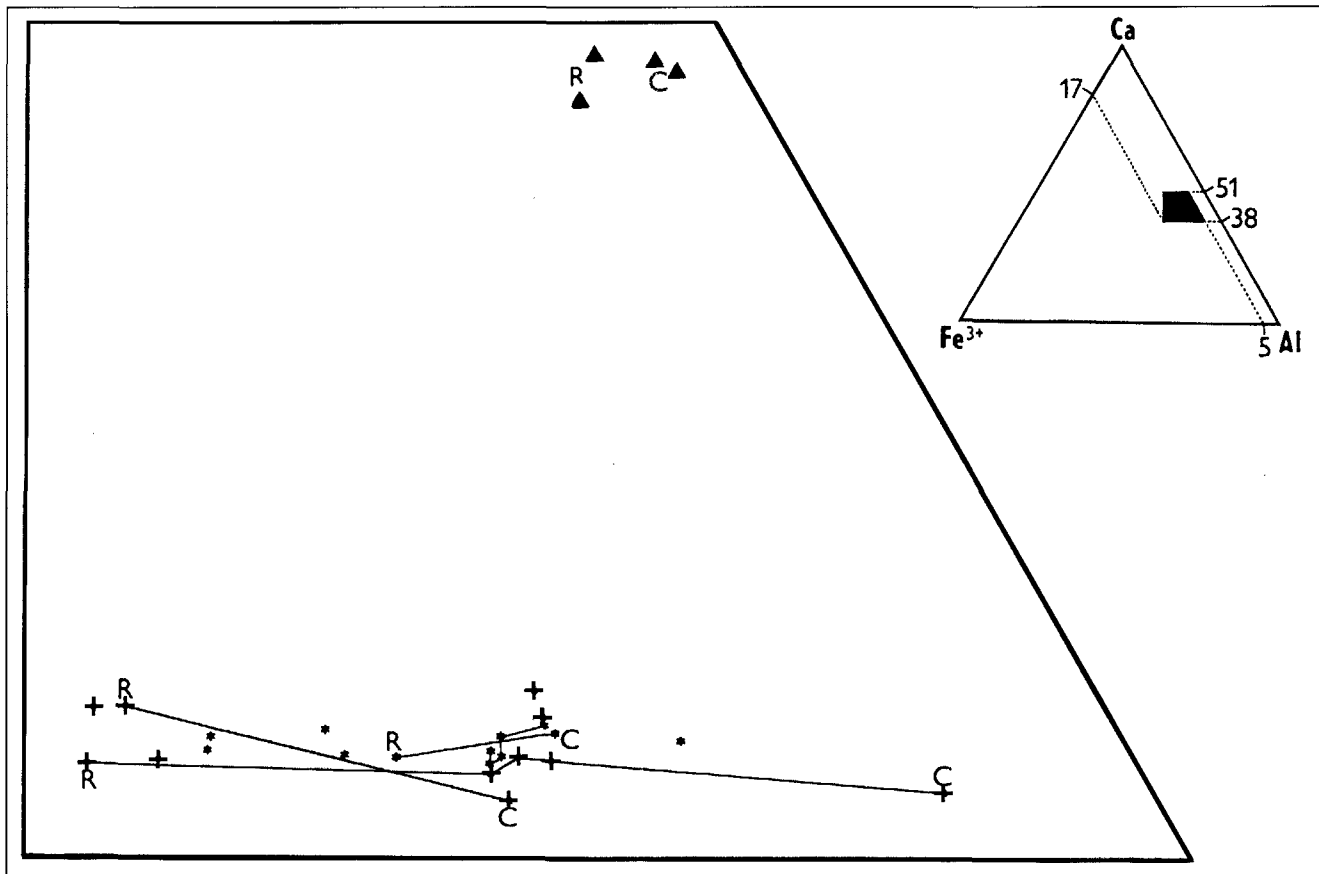


Fig. 2.
Chemical composition of epidote and prehnite, Ca - Al - Fe^{3+} diagram.
C = core, R = rim. * = epidote from the paragenetic type A; + = epidote from the paragenetic type P; ▲ = prehnite.

sulzbachtal (SEEMANN et al., 1990) and in Krásné near Sobotín (BERNARD, 1981) have not been observed in any studied samples and they have not been reported in previous studies (KRETSCHMER, 1895, 1911; NEUWIRTH, 1905; BURKART 1953, KRUŠA 1966).

Study of the relations between individual minerals using a binocular and petrographic microscopes indicates, that all earlier-formed minerals have nearly apparent euhedral forms compared with the younger overgrowth. Some mineral pairs, such as diopside-epidote, epidote-albite, laumontite-stilbite, epidote-prehnite show distinct evidences of these textural relations, even than most of them may coexist, e.g. epidote-prehnite (LIOU et al. 1983) or epidote-albite (APTED & LIOU, 1983). The apparent non-equilibrium relations between pair minerals, epidote-actinolite and albite-prehnite were observed. Both minerals of the individual pair are rarely associated although they formed in a similar temporal event of a fissure formation.

3. Chemical composition

The fissure minerals were analysed by the electron microprobe JEOL JXA 50-A in the Geological Institute of the Czech Academy of Sciences in Praha. Synthetic compounds and natural minerals were used as standards. The data were reduced using the program published by JUREK & ŠKVÁRA, 1973; analysts: A. LANGROVÁ and V. ŠREIN.

Chemical composition of epidote varies in a wide range of the mole fraction of $\text{Ca}_2\text{Fe}_3\text{Si}_3\text{O}_{12}(\text{OH})-\text{X}_{\text{Fe}}$. The epidote crystals from the paragenetic type P show significant zoning (Tab. 1, Fig. 2); the X_{Fe} value increases from core to

rim and such increase is apparently discontinuous. On the other hand, the epidote crystals of the type A do not show so conspicuous zoning; compositions are rather continuous, but exhibit similar zoning trend (Fig. 2). Chemical composition of epidote from some metabasic rocks of the Sobotín massif (FIALA et al., 1980; BUKOVANSKÁ, 1990) is comparable with the epidotes from fissures.

Prehnite is chemically more uniform; however, the X_{Fe} value increases slightly from core to rim similarly as in epidotes (see Fig. 2). Amphiboles (actinolite and asbestos) show very similar composition (Tab. 2), comparable with actinolite from albite-epidote amphibolite of the Sobotín massif (FIALA et al. 1980). Apatite from the paragenetic

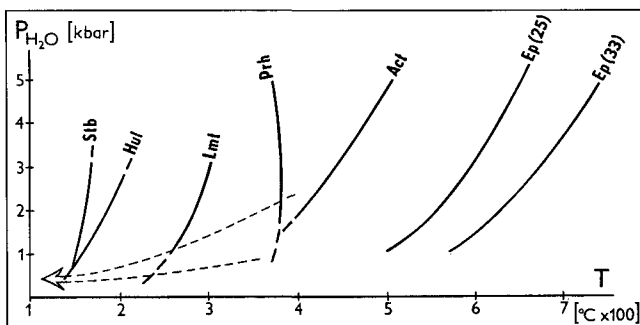


Fig. 3.
P-T diagram depicted equilibrium reactions for selected minerals.
Data were taken from LIOU (1971a, 1971b, 1973); CHO et al., (1987) and MARAYUMA et al. (1983).
Stb = stilbite, Hul = heulandite, Lmt = laumontite, Prh = prehnite, Act = actinolite, Ep = epidote; numbers in parentheses = pistacite content in epidote.

| | 1. | 2. | 3. | 4. | 5. | 6. | 7. | 8. | 9. |
|----------------------------------|-------|-------|-------|-------|-------|-------|-------|-------|-------|
| SiO ₂ | 38.36 | 38.04 | 37.94 | 37.46 | 38.26 | 37.07 | 37.11 | 37.73 | 37.30 |
| TiO ₂ | 0.08 | 0.20 | 0.22 | 0.27 | 0.32 | 0.12 | 0.08 | 0.06 | 0.09 |
| Al ₂ O ₃ | 25.45 | 24.53 | 24.60 | 24.59 | 23.12 | 27.82 | 24.96 | 21.53 | 21.49 |
| Fe ₂ O ₃ * | 8.78 | 10.59 | 10.83 | 10.05 | 12.25 | 6.50 | 10.41 | 14.89 | 14.57 |
| MnO | 0.17 | 0.11 | 0.08 | 0.04 | 0.24 | 0.03 | 0.15 | 0.02 | 0.08 |
| MgO | 0.08 | 0.02 | 0.01 | 0.02 | 0.02 | 0.00 | 0.02 | 0.00 | 0.04 |
| CaO | 23.52 | 23.68 | 23.48 | 23.70 | 23.15 | 23.49 | 23.64 | 23.14 | 23.50 |
| Na ₂ O | 0.00 | 0.00 | 0.00 | 0.02 | 0.01 | 0.00 | 0.01 | 0.00 | 0.03 |
| K ₂ O | 0.02 | 0.01 | 0.01 | 0.00 | 0.02 | 0.02 | 0.01 | 0.02 | 0.01 |
| Total | 96.46 | 97.18 | 97.17 | 96.15 | 97.39 | 95.05 | 96.39 | 97.39 | 97.11 |
| | | | | | | | | | |
| Si | 3.050 | 3.025 | 3.018 | 3.009 | 3.051 | 2.970 | 2.979 | 3.038 | 3.018 |
| Ti | 0.005 | 0.012 | 0.013 | 0.016 | 0.019 | 0.007 | 0.005 | 0.004 | 0.005 |
| Al | 2.385 | 2.299 | 2.306 | 2.328 | 2.173 | 2.626 | 2.361 | 2.043 | 2.049 |
| Fe ³⁺ | 0.525 | 0.634 | 0.648 | 0.607 | 0.739 | 0.392 | 0.629 | 0.902 | 0.887 |
| Mn | 0.011 | 0.007 | 0.005 | 0.003 | 0.016 | 0.002 | 0.010 | 0.001 | 0.005 |
| Mg | 0.009 | 0.002 | 0.001 | 0.002 | 0.002 | 0.000 | 0.002 | 0.000 | 0.005 |
| Ca | 2.003 | 2.017 | 2.001 | 2.039 | 1.973 | 2.016 | 2.033 | 1.996 | 2.037 |
| Na | 0.000 | 0.000 | 0.000 | 0.003 | 0.002 | 0.000 | 0.003 | 0.000 | 0.005 |
| K | 0.002 | 0.001 | 0.001 | 0.000 | 0.002 | 0.002 | 0.001 | 0.002 | 0.001 |
| Sum | 7.990 | 7.997 | 7.993 | 8.007 | 7.977 | 8.015 | 8.023 | 7.986 | 8.012 |

Table 1. Representative analyses of epidote (+ = Total Fe as Fe₂O₃). 1 = associated with actinolite (sample 3A); 2,3,4 = unzonal associated with albite, from core to rim (sample 8A); 5 = associated with K-feldspar (sample 6A); 6,7,8 = zonal crystal from core to rim (sample 11P); 9 = associated with prehnite (sample 11P). Analyses No. 1 to 5 = paragenetic type A; analyses No. 6 to 9 = paragenetic type P.

| | 1. | 2. | 3. | 4. | 5. | 6. | 7. | 8. | 9. |
|----------------------------------|-------|--------|--------|--------|--------|--------|--------|-------|-------|
| SiO ₂ | 53.20 | 53.63 | 52.01 | 54.63 | 54.55 | 54.43 | 53.87 | 43.15 | 42.75 |
| TiO ₂ | 0.08 | 0.05 | 0.09 | 0.05 | 0.18 | 0.11 | 0.07 | 0.06 | 0.04 |
| Al ₂ O ₃ | 1.20 | 1.50 | 3.11 | 1.58 | 2.47 | 2.38 | 1.49 | 20.90 | 20.32 |
| Fe ₂ O ₃ * | 0.00 | 0.00 | 0.00 | 0.00 | 0.00 | 0.00 | 0.00 | 4.34 | 5.46 |
| FeO** | 7.33 | 5.36 | 12.21 | 11.70 | 9.94 | 10.40 | 12.18 | 0.00 | 0.00 |
| MnO | 0.19 | 0.55 | 0.40 | 0.46 | 0.46 | 0.34 | 0.63 | 0.00 | 0.09 |
| MgO | 13.20 | 13.99 | 14.87 | 15.48 | 16.68 | 16.21 | 16.03 | 0.00 | 0.00 |
| CaO | 23.84 | 24.62 | 12.55 | 12.52 | 12.74 | 12.73 | 12.60 | 26.51 | 26.22 |
| Na ₂ O | 0.42 | 0.35 | 0.61 | 0.21 | 0.35 | 0.36 | 0.18 | 0.00 | 0.00 |
| K ₂ O | 0.02 | 0.02 | 0.17 | 0.06 | 0.14 | 0.06 | 0.06 | 0.02 | 0.04 |
| Total | 99.48 | 100.07 | 96.02 | 96.69 | 97.51 | 97.02 | 97.11 | 94.98 | 94.92 |
| | 6 | 6 | 23 | 23 | 23 | 23 | 23 | 11 | 11 |
| Si | 1.988 | 1.980 | 7.643 | 7.901 | 7.775 | 7.805 | 7.802 | 3.030 | 3.015 |
| Ti | 0.002 | 0.001 | 0.010 | 0.005 | 0.019 | 0.012 | 0.008 | 0.003 | 0.002 |
| Al | 0.053 | 0.065 | 0.539 | 0.269 | 0.415 | 0.402 | 0.254 | 1.730 | 1.696 |
| Fe ³⁺ | 0.000 | 0.000 | 0.000 | 0.000 | 0.000 | 0.000 | 0.000 | 0.229 | 0.290 |
| Fe ²⁺ | 0.229 | 0.165 | 1.500 | 1.415 | 1.185 | 1.247 | 1.475 | 0.000 | 0.000 |
| Mn | 0.006 | 0.017 | 0.050 | 0.056 | 0.056 | 0.041 | 0.077 | 0.000 | 0.005 |
| Mg | 0.738 | 0.770 | 3.257 | 3.337 | 3.543 | 3.464 | 3.460 | 0.000 | 0.000 |
| Ca | 0.953 | 0.974 | 1.976 | 1.940 | 1.945 | 1.956 | 1.955 | 1.994 | 1.981 |
| Na | 0.030 | 0.025 | 0.174 | 0.059 | 0.097 | 0.100 | 0.051 | 0.000 | 0.000 |
| K | 0.001 | 0.001 | 0.032 | 0.011 | 0.025 | 0.011 | 0.011 | 0.002 | 0.004 |
| Sum | 4.000 | 3.998 | 15.181 | 14.993 | 15.060 | 15.038 | 15.093 | 6.988 | 6.993 |

Table 2. Representative analyses of pyroxene, amphiboles and prehnite (+ = Total Fe as Fe₂O₃, ++ = Total Fe as FeO). 1 = diopside (sample 7A); 2 = diopside (sample 10P); 3,4 = actinolite associated with albite (sample 1A); 5 = actinolite associated with epidote (sample 3A); 6,7 = actinolite asbestos (sample 13P); 8,9 = prehnite from core to rim (sample 11P). Analyses No. 1,3,4,5 = paragenetic type A; analyses No. 2,6 to 9 = paragenetic type P.

| | 1. | 2. | 3. | 4. | 5. | 6. | 7. | 8. |
|--------------------------------|-------|--------|--------|-------|-------|-------|--------|--------|
| SiO ₂ | 68.40 | 68.94 | 69.09 | 64.08 | 64.43 | 31.32 | 53.82 | 58.85 |
| TiO ₂ | 0.00 | 0.00 | 0.00 | 0.05 | 0.05 | 37.58 | 0.00 | 0.00 |
| Al ₂ O ₃ | 18.85 | 19.57 | 19.54 | 17.75 | 18.00 | 0.98 | 21.27 | 16.81 |
| FeO* | 0.00 | 0.00 | 0.00 | 0.00 | 0.00 | 0.46 | 0.00 | 0.00 |
| MnO | 0.00 | 0.05 | 0.00 | 0.00 | 0.01 | 0.11 | 0.00 | 0.02 |
| MgO | 0.00 | 0.00 | 0.00 | 0.00 | 0.00 | 0.00 | 0.14 | 0.03 |
| CaO | 0.00 | 0.02 | 0.00 | 0.00 | 0.00 | 29.25 | 11.19 | 7.90 |
| Na ₂ O | 11.76 | 11.81 | 11.81 | 0.16 | 0.09 | 0.00 | 0.01 | 1.12 |
| K ₂ O | 0.03 | 0.00 | 0.03 | 16.54 | 16.62 | 0.02 | 0.93 | 0.28 |
| Total | 99.04 | 100.39 | 100.47 | 98.58 | 99.20 | 99.72 | 87.36 | 85.01 |
| | 8 | 8 | 8 | 8 | 8 | 5 | 16 | 16 |
| Si | 3.014 | 2.998 | 3.001 | 3.010 | 3.006 | 1.025 | 6.130 | 6.738 |
| Ti | 0.000 | 0.000 | 0.000 | 0.002 | 0.002 | 0.925 | 0.000 | 0.000 |
| Al | 0.979 | 1.003 | 1.000 | 0.983 | 0.990 | 0.038 | 2.855 | 2.268 |
| Fe ²⁺ | 0.000 | 0.000 | 0.000 | 0.000 | 0.000 | 0.013 | 0.000 | 0.000 |
| Mn | 0.000 | 0.002 | 0.000 | 0.000 | 0.000 | 0.003 | 0.000 | 0.002 |
| Mg | 0.000 | 0.000 | 0.000 | 0.000 | 0.000 | 0.000 | 0.024 | 0.005 |
| Ca | 0.000 | 0.001 | 0.000 | 0.000 | 0.000 | 1.026 | 1.365 | 0.969 |
| Na | 1.005 | 0.996 | 0.994 | 0.015 | 0.008 | 0.000 | 0.002 | 0.249 |
| K | 0.002 | 0.000 | 0.002 | 0.991 | 0.989 | 0.001 | 0.135 | 0.041 |
| Sum | 5.000 | 5.000 | 4.997 | 6.001 | 4.995 | 3.031 | 10.511 | 10.272 |

type P corresponds to fluorapatite ($F_2 = 1.64$ wt-%, $H_2O = 0.43$ wt-%; personal. comm. Dr. P. Povondra). Albite and K-feldspar are close to their end-member compositions (>99 %, Tab. 3).

Composition of individual minerals from both paragenetic types differs slightly except for the X_{Fe} variation in epidotes. Diopside from the type A contains higher FeO and lower MnO; epidote from the type A appears to be higher in MnO and TiO₂.

4. Discussion

Both paragenetic types of the fissure mineralization are irregularly distributed within a small area. They appear to have formed at similar P-T conditions. In this case, reactions for appearance of selected minerals were depicted in a single schematic P-T diagram (Fig. 3). The upper temperature limit of fissure formation could not be higher than the peak temperature for regional metamorphism of the studied area at about 350 to 425°C (FIALA et al., 1980). The assumed decrease in P-T conditions during the fissure formation are schematically shown by the dashed arrow in Fig. 3. The lower limit inferred from the stilbite formation seems to be below 150°C and P_{fluid} lower than 1 kbar.

Different mineral parageneses in the studied fissures reflect difference in chemical composition of fluid derived from closely adjacent rocks. The paragenetic type A characterized by very common albite, epidote and less

Table 3.
Representative analyses of feldspars, sphene and zeolites (+ = Total Fe as FeO).
1 = albite associated with actinolite (sample 1A); 2 = albite associated with K-feldspar (sample 2A); 5 = K-feldspar associated with prehnite (sample 9P); 6 = sphene (sample 4A); 8 = stilbite (sample 4A). Analyses No. 1 to 4 and 6 to 8 = paragenetic type A; analysis No. 5 = paragenetic type P.

common actinolite may have been associated with fluids of high Na activity and most likely low fO_2 in a comparison with the paragenetic type P. Small variation in the X_{Fe} value and weak to negligible zoning of the epidote crystals support this conclusion (LIOU, 1973, 1990). It should be noted that composition of a nearly unzoned epidote could be also buffered by associated minerals, especially actinolite and albite. An occurrence of diopside and actinolite and/or actinolite + K-feldspar supports very low CO₂ activity in the fluid (CHO et al., 1988). Mineral paragenesis of the type P is represented by very common prehnite and epidote and by absence of albite and actinolite. The epidote crystals exhibit significant discontinuous zoning suggested relatively higher fO_2 (LIOU, 1973, 1990). Nevertheless, this zoning could also be influenced by other factors including change in temperature and in pH (LIOU, 1990). Common occurrence of prehnite and entire absence of calcite and chlorite indicate very low X_{CO_2} and perhaps low NaCl in the fluids (RICE, 1983; CHO & LIOU, 1987; CHO et al., 1988). This is supported by an absence of albite. Chemical composition of fluorapatite from the type P exhibits low CO₂ activity.

Unfortunately, no iron oxides such as hematite and magnetite were found in the studied fissures, hence more precise fO_2 estimate could not be made.

The observed mineral assemblages, paragenetic relations and chemical composition of minerals are very similar to those from metabasites of the greenschist to zeolite facies (MARAYUMA et al., 1983; LIOU et al., 1983; CHO et al., 1986; CHO & LIOU, 1987; LEVI et al., 1989) and partly also in

the epidote-bearing veins in an active geothermal system of the Salton Sea, California (CARUSO et al.; 1988, CHO et al., 1988). However, textural relations between individual minerals in fissures in a macroscopic scale are rather different from those in thin sections of metabasites.

Acknowledgement

The authors express thanks to Prof. J.G. Liou (Stanford University, California) for his careful review of an early version of this manuscript and helpful suggestions.

References

- APTED, M.J. & LIOU, J.G. (1983): Phase relations among green-schists, epidote amphibolite and amphibolite in a basaltic system. – Am. J. Sci., **283A**, 328–354, New Haven.
- BERNARD, J.H. (1981): Minerals of the Alpine veins and of similar assemblages. – In: BERNARD, J.H. (ed): Mineralogy of Czechoslovakia, 405–419, Academia Praha (in Czech).
- BUKOVANSKÁ, M. (1990): Epidote occurrences in Alpine type dykes and ultrabasic rocks of the Sobotín (Zöptau) amphibolite massif, Czechoslovakia. – Mitt. Österr. Min. Ges., **135**, 13–14, Wien.
- BURKART, E. (1953): Mährens Minerale und ihre Literatur. – 1004 S., Nakl. ČSAV Praha.
- CARUSO, L.J., BIRD, D.K., CHO, M. & LIOU, J.G. (1988): Epidote-bearing veins in the State 2–14 drill hole: Implications for hydrothermal fluid composition. – J. Geophys. Res., **93**, 13123–13133, Washington.
- CHO, M. & LIOU, J.G. (1987): Prehnite-Pumpellyite to greenschist facies transition in the Karmutsen metabasites, Vancouver Islands, British Columbia. – J. Petrology, **28**, 417–443, Oxford.
- CHO, M., LIOU, J.G. & BIRD, D.K. (1988): Prograde phase relations in the State 2–14 well metasandstones, Salton Sea geothermal field, California. – J. Geophys. Res., **93**, 13081–13103, Washington.
- CHO, M., LIOU, J.G. & MARAYUMA, S. (1986): Transition from the zeolite to prehnite-pumpellyite facies in the Karmutsen metabasites, Vancouver Islands, British Columbia. – J. Petrology, **27**, 467–494, Oxford.
- CHO, M., MARAYUMA, S. & LIOU, J.G. (1987): An experimental investigation of heulandite-laumontite equilibrium at 1000 to 2000 bar P_{fluid}. – Contrib. Mineral. Petrol., **97**, 43–50, New York.
- FIALA, J., JELÍNEK, E., POUBA, Z., POUBOVÁ, M. & SOUČEK, J. (1980): The geochemistry of the ultrabasic rocks of the Sobotín amphibolite massif (Czechoslovakia). – N. Jb. Miner. Abh., **137**, 257–281. Stuttgart.
- JUREK, K. & ŠKVÁRA, F. (1973): Quantitative X-ray microanalyses of silicates II. – Silikáty, **17**, 349–354, Praha (in Czech).
- KRETSCHMER, F. (1895): Die Mineralfundstätten von Zöptau und Umgebung. – Tschermaks Min. Pet. Mitt., 156–187, Wien.
- KRETSCHMER, F. (1911): Das metamorphe Diorit- und Gabbromassiv in der Umgebung von Zöptau (Mähren). – Jb. Geol. R.-A., **61**, 53–179, Wien.
- KRUŠA, T. (1966): Mährens Minerale und ihre Literatur 1940–1965. – 379 S., Moravian Museum, Brno.
- LEVI, B., AQUIRRE, L., NYSTRÖM, J.O., PADILLA, H. & VERGARA, M. (1989): Low-grade metamorphism in the Mesozoic-Cenozoic volcanic sequence of the Central Andes. – J. Metam. Geol., **7**, 487–495. Oxford.
- LIOU, J.G. (1971a): Synthesis and stability relations of prehnite, Ca₂Al₂Si₃O₁₀(OH)₂. – Amer. Mineralogist, **56**, 507–531, Washington.
- LIOU, J.G. (1971b): Stabilities of laumontite, wairakite, lawsonite and related minerals in the System CaAl₂Si₂O₈ – SiO₂ – H₂O. – J. Petrology, **12**, 379–411, Oxford.
- LIOU, J.G. (1973): Synthesis and stability relations of epidote, Ca₂Al₂FeSi₃O₁₂(OH). – J. Petrology, **14**, 381–413, Oxford.
- LIOU, J.G. (1990): Stabilities and compositional variations of natural epidotes. – Mitt. Österr. Min. Ges., **135**, 51–53, Wien.
- LIOU, J.G., KIM, H.S. & MARAYUMA, S. (1983): Prehnite-epidote equilibria and their petrologic applications. – J. Petrology, **24**, 321–342, Oxford.
- MARAYUMA, S., SUZUKI, K. & LIOU, J.G. (1983): Greenschist-ampibolite transition equilibria at low pressure. – J. Petrology, **24**, 583–604, Oxford.
- NEUWIRTH, V. (1904): Der Albit von Zöptau in Mähren. – Z. Mähr. Landesmuseum, 39–54, Brünn.
- NEUWIRTH, V. (1905): Die paragenetischen Verhältnisse der Minerale im Amphibolitgebiet von Zöptau. – Mähr. Landesmuseum, 120–180, Brünn.
- NOVÁK, M. (1990): Formation of epidote and associated minerals in fissures from Pfarrerb near Sobotín, northern Moravia, Czechoslovakia. – Mitt. Österr. Min. Ges., **135**, 62–64, Wien.
- RATH, G. von (1881): Mineralien von Zöptau. – Zeitschr. f. Kristallogr., **5**, 253–267, Wien.
- RENÉ, M. (1983): Geochemistry and petrology of metapelites in the envelope of the core of the Desná Dome in northern Moravia. – Čas. Mineral. Geol., **28**, 277–286, Praha (in Czech with English summary).
- RICE, J.M. (1983): Metamorphism of rodingites; Part I. Phase equilibria in a portion of the System CaO–MgO–Al₂O₃–SiO₂–CO₂–H₂O. – Amer. J. Sci., **283A**, 121–150, New Haven.
- SEEMANN, R., KOLLER, F., GRUNDMANN, G., BRANDSTÄTTER, F. & STEININGER, H. (1990): Historische Kupferlagerstätte „Hochfeld“ und Epidot-Fundstelle „Knappenwand“, Untersulzbachtal. – Mitt. Österr. Min. Ges., **135**, 95–117, Wien.
- ZEPHAROVICH, V. (1865): Epidot von Zöptau in Mähren. – Sitzungsber. Königl. Böh. Ges. Wiss., **63**, Prag.

Received 20. 12. 1990 * Accepted 4. 2. 1992